01 Jan 2020

Mobile-manipulating UAVs for Sensor Installation, Bridge Inspection and Maintenance

Paul Oh

Blake Helmet

Dongbin Kim

FINAL REPORT

#INSPIRE-004

GRANT NO: 69A3551747126
GRANT PERIOD: 11/30/16 – 09/30/22
PROJECT PERIOD: 03/31/17 – 03/31/20

Inspecting and Preserving Infrastructure through Robotic Exploration (INSPIRE)

Tier 1 University Transportation Center Sponsored by the Office of the Assistant Secretary for Research and Technology (OST-R)

Project/Report Title:	**Mobile-manipulating UAVs for Sensor Installation, Bridge Inspection and Maintenance**
Consortium Member:	University of Nevada Las Vegas
Principal Investigator:	Paul Oh
Co-Principal Investigator(s):	
Report Authors:	Paul Oh, Blake Helmet, and Dongbin Kim

Missouri S&T · The City College of New York · Georgia Tech · CU · UNLV · N · East Central College · Lincoln · Ozarks Technical Community College · St. Louis Community College

DISCLAIMER

The contents of this report reflect the views of the authors, who are responsible for the facts and the accuracy of the information presented herein. This document is disseminated in the interest of information exchange. The report is funded, partially or entirely, by a grant from the U.S. Department of Transportation's University Transportation Centers Program. However, the U.S. Government assumes no liability for the contents or use thereof.

TECHNICAL REPORT DOCUMENTATION PAGE

1. Report No. INSPIRE-004	**2. Government Accession No.** (blank)	**3. Recipient's Catalog No.** (blank)
4. Title and Subtitle Augmenting Bridge Inspection with Augmented Reality and Haptics-based Aerial Manipulation		**5. Report Date** 03/31/2020 **6. Performing Organization Code** (blank)
7. Author(s) Paul Oh, Blake Helmet and Dongbin Kim		**8. Performing Organization Report No.** (blank)
9. Performing Organization Name and Address University of Nevada Las Vegas 4505 S. Maryland Parkway, Mailstop 454009 Las Vegas, NV, 89154		**10. Work Unit No.** (blank) **11. Contract or Grant No.** USDOT #69A3551747126
12. Sponsoring Agency Name and Address Office of the Assistant Secretary for Research and Technology U.S. Department of Transportation 1200 New Jersey Avenue, SE Washington, DC 20590		**13. Type of Report and Period Covered** Final Report Period: 03/31/2017 – 03/31/2020 **14. Sponsoring Agency Code** (blank)
15. Supplementary Notes The investigation was conducted under the auspices of the INSPIRE University Transportation Center.		

16. Abstract

A parallel mechanism and smart gripper was designed and mounted on a rotorcraft drone to act as a robotic arm and hand. This empowers the drone to perform aerial manipulation and execute bridge maintenance. Hosing, drilling, and epoxying serve as case studies to test-and-evaluation and verify-and-validate the design. The approach, tasks, and findings are presented and show that the case studies are realizable. Conclusions and recommendations point to employing haptics-based human-in-the-loop approaches that can increase the scope of repair work involved in bridge maintenance.

17. Key Words Bridge Maintenance, Drones, Manipulation	**18. Distribution Statement** No restrictions. This document is available to the public.	
19. Security Classification (of this report) Unclassified	**20. Security Classification (of this page)** Unclassified	**21. No of Pages** 30

Form DOT F 1700.7 (8-72) Reproduction of form and completed page is authorized.

EXECUTIVE SUMMARY

In this project, an aerial manipulator was designed for bridge maintenance tasks. The manipulator consists of a robotic arm, smart gripper, and underlying null-space impedance-based control law. A parallel mechanism (Stewart Platform) was used to design the robotic arm. This design is novel and provides six degrees-of-freedom range at a reduced weight. Furthermore as a parallel mechanism, it easily mounts on the belly of a conventional rotorcraft drone and folds flat. This "tuck-and-stow" feature ensures the arm does not interfere with the aircraft take-off and landing. Proximity and ambient light sensors were embedded into a 4-bar mechanism to yield a smart gripper. This design acts as a hand that can sense object shape and size. The underlying control law ensures that the drone remains stable while perform aerial manipulation.

Tasks like hosing, drilling and epoxying served as technical design requirements for the aerial manipulator. These tasks are often performed in bridge maintenance. These tasks also generate reaction forces and torques that could destabilize aerial manipulation. For hosing, the gripping pose (position and orientation) was identified that ensured the drone remained stable. Demonstrations of hosing a bridge deck and its side validated the design. For drilling, different surfaces, drill bits, and drill rotational speed yield different reaction forces and torques. Thus, a priori knowledge is important to successfully perform autonomous drilling with aerial manipulation. A novel approach was used that showed promise; a human-in-the-loop method was employed to remotely tele-operate aerially manipulated drilling. Here, a haptic device provided the operator with force feedback. The operator's experience served in identifying drilling feed rate and rotational speed. Filling cracks with epoxy was initiated. However the goal of deck repair also requires roughening the surface before and spreading the epoxy after a crack is filled. To fully perform epoxying, the reaction forces and torques involved in surface-roughening and epoxy-spreading are needed a priori. However, the human-in-the-loop haptics-based approach has promise in performing this. Coupling force feedback with immersive technologies like virtual-reality and augmented-reality would have even more promise. This coupling aligns with the "future of work" that augments bridge maintenance crews with new skills to perform an even broader range of tasks.

ACKNOWLEDGMENT

Financial support for this INSPIRE UTC project was provided by the U.S. Department of Transportation, Office of the Assistant Secretary for Research and Technology (USDOT/OST-R) under Grant No. 69A3551747126 through INSPIRE University Transportation Center (http://inspire-utc.mst.edu) at Missouri University of Science and Technology. The views, opinions, findings and conclusions reflected in this publication are solely those of the authors and do not represent the official policy or position of the USDOT/OST-R, or any State or other entity.

TABLE OF CONTENTS

1. DESCRIPTION OF THE PROBLEM

The U.S. roadway transportation system is composed of nearly 600,000 bridges and 6,300,000 kilometers of streets and highways. As transportation demand continues to grow, highways and bridges must be maintained and operated efficiently. This ensures a steady growth of the nation's economy. Bridge maintenance often requires closing traffic lanes, requires large overhead in equipment setup, and endangers workers. One potential resource is an unmanned aerial vehicle (drone) to accelerate maintenance. Maintenance crews can remotely inspect bridges using the aircraft's onboard optical sensors like cameras and rangefinders. This is approach continues to be an applied research area. Effort has mainly focused on stability control, especially against gust and wind shear that is common near bridge decks. Aerial manipulation is a disruptive approach where manipulators are mounted on the drone. The notion is that such robotic arms and hands enable the vehicle to *actively interact* with their environment (like drill surfaces, apply epoxies, and clean decks). This is a paradigm shift where today's drones just *passively surveil* the environment rather than do physical work.

2. APPROACH

Equipping a drone with robotic arms and hands would enable the vehicle to perform maintenance tasks on bridges. Some notional examples include carrying and manipulating: hoses to wash bridge decks; drills to prep surfaces for inserting new bolts and rivets; brushes to sweep; and applicators to epoxy cracks. Such aerial manipulation is a relatively new but growing area of research. The *critical gap* that prevents research advancement is stability. Called under-actuation, the challenge is to keep the vehicle fixed in space even when the arms move or interact with objects; the flight controller must counteract reaction forces and torques.

2.1 Approach - Impedance-based Manipulator Control (Year 1):

Manipulators on free-floating platforms are not new. Underwater rovers equipped with one or multiple manipulators have been used for marine salvage operations. Spacecraft like the shuttle also come equipped with an arm to perform missions like satellite repair. For these under-actuated vehicles, the "best practice" has been to apply null-space based impedance control. When the reaction forces and torques are fully known, the control design is straight-forward.

Another challenge in aerial manipulation is weight and size. The performance of a robotic arm and hand is characterized by the number of degrees-of-freedom (DOF) and workspace reach. Typically full dexterity demands 6-DOF and current aerial manipulation research employs a serial-linked configuration; each DOF is powered by a motor. The net effect is that the arm has limited torque (using small and light-weight motors) or workspace (links are short).

2.2 Approach – Stewart-based Manipulator Design (Year 1):

Parallel mechanisms are often used to overcome weight and workspace limitations. For example, the Stewart Platform is often used in commercial aircraft simulators. Here; the mock-up cockpit sits on top of the platform. The platform heaves and sways to emulator aircraft motions. An inverted Stewart Platform configuration is also seen in assembly lines as 6-DOF pick-and-place manipulators. For aerial manipulation a parallel mechanism based approach will be used. The resulting arm would have the 6-DOF needed for dexterity but employ fewer motors. Moreover, the arm's kinematics naturally lends itself to folding flat. The arm can "tuck-and-stow" under the drone's belly and not interfere with vehicle take-off and landing.

Beyond workspace reach, robotic hands are needed to dexterously manipulate objects and tools. Hand design and grasping remains an open research area in robotics.

2.3 Approach – Smart Gripper (Year 2):

Proximity and ambient light sensors can be embedded in the gripper. The latter emits infrared light on objects and the latter employs time-of-flight measurements on the reflection. Together, one can design a low-weight sensor package that can quickly yield object size and shape without large computation overhead. This package will be embedded on a gripper. The gripper will be a 4-bar linkage design to demonstrate efficacy for aerial manipulation.

Crack repair in bridge decks involves tasks like: prep-work by hosing or blowing debris from the crack; laying out work perimeter by assessing the surface surrounding the crack; filling the crack with epoxy;

scrubbing the hardened epoxy with wire brushes; and clean-up. All these tasks involve manipulation and hence serve as a case study to define requirements and demonstrate efficacy.

2.4 Approach – Hosing, Drilling, and Epoxying (Year 3):

To demonstrate the aerial manipulator's stability and application to deck maintenance, hosing and drilling were selected. Here, the jet stream from the hose and drilling into concrete generate reaction forces and torques on the aircraft and its manipulator. Epoxying would be another application to demonstrate efficacy of the design and promise for bridge maintenance.

3 METHODOLOGY

All the aforementioned approaches leveraged the lab's Sensors Integrated Systems Test Rig (SISTR). From 2003 to 2018, grants from the National Science Foundation (NSF) funded this infrastructure for the testing-and-evaluation (T&E) of drones and aerial manipulation. SISTR is a 6 degree-of-freedom (DOF) gantry. The drone is mounted on the gantry's end-effector (Figure 3). A high-fidelity math model of the aircraft's dynamics is used to move the drone within the gantry's workspace (Figure 4). A real-world environment is then emulated inside the workspace. The resulting hardware-in-the-loop system allows one to analytically design controllers, tune sensors, and measure task performance. Validation-and-verification (V&V) is then performed in the lab's motion-capture (mo-cap) arena. Here, the real-world environment is recreated in the arena. The untethered drone repeats tasks to ensure performance in SISTR is reproducible in free-flight including outdoors.

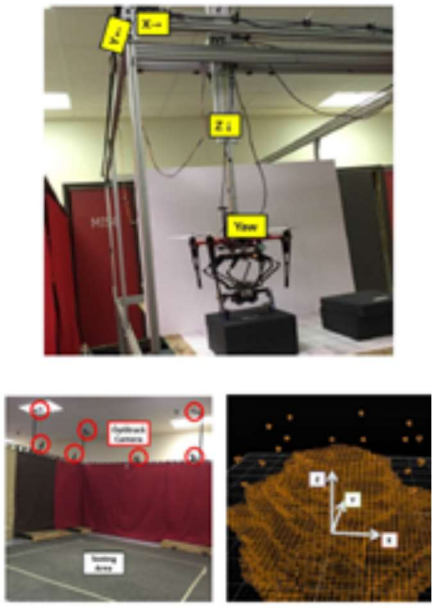

Figure 3: Drone (with aerial manipulator) mounted in SISTR for T&E and free-flying in mo-cap arena for V&V

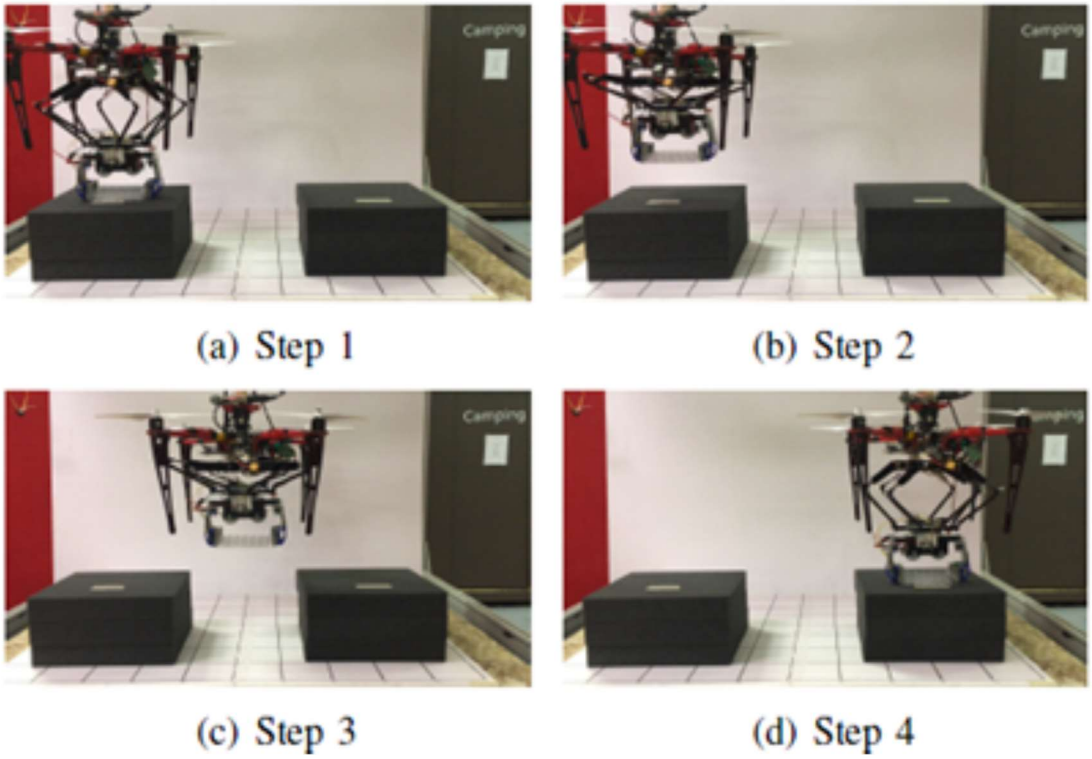

Figure 4: Close-up of aerial manipulator in SISTR perform pick-and-place sequence.

3.1 Task 1: Impedance-based Controller and Stewart-Based Parallel Manipulator (Year 1)

The flight controller was implemented using a cascade structure[1]. The drone's avionics (e.g. Pixhawk embedded micro-controller) is an inner-loop. To mitigate outside disturbances like reaction forces and torques, a 100 Hz outer-loop compensator was designed to implement proportional-derivative control (Figure 5). In flight, the drone and reference positions are compared to form the error $e(t)$. After compensation, the signal $u(t)$ is formed and converted into a reference speed $v(t)$ in the inner loop as an input for the internal controller.

[1] Detailed derivations can be found in accepted paper: Kim, D. and Oh, P.Y., "Testing-and-Evaluation Platform for Haptics-based Aerial Manipulation with Drones," American Control Conference (ACC), Denver, CO, July 2020.

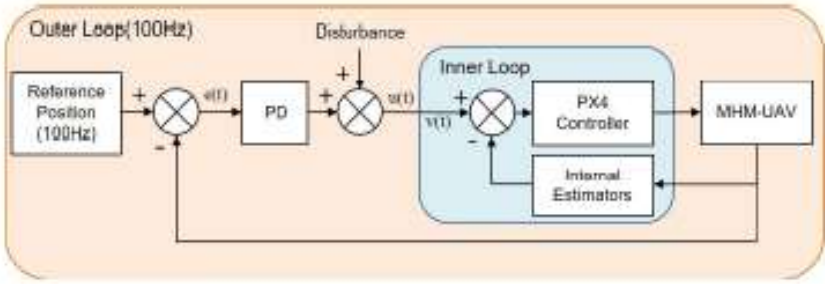

Figure 5: Cascade controller block diagram.

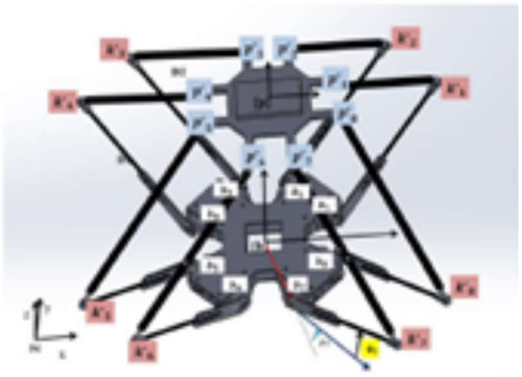

Figure 6: Image of CAD model

Figure 7: Prototype Parallel Manipulator

Leg(i)	$\psi_{bi}(radians)$	$\gamma_i(radians)$	$\psi_{pi}(radians)$
1	0.3658	0.4196	0.2782
2	1.2050	0.4196	1.2926
3	1.9336	0.4196	1.8490
4	2.7758	0.4196	2.8634
5	3.5074	0.4196	3.4198
6	4.3466	0.4196	4.4342
7	5.0781	0.4196	4.9906
8	5.9194	0.4196	6.0050

Figure 8: Prototype parallel manipulator dimensions

Figures 6, 7, and 8 show the CAD design, prototype and ranges of motion (left, center, and right respectively)[2]. The manipulator uses mini RC servos yielding a 0.7 kilogram 6-DOF. The mechanism has 8 legs. Each leg has one driven revolute joint and two spherical joints (8-RSS configuration). Each leg, i, is attached to a servo on the base by a revolute joint. The servo drives a fixed length link, $D1$, to an angle ϑ_i from the plane of the base. The $D1$ link is connected to a second fixed length link, $D2$, via a spherical "knee" joint, and the other end of the $D2$ link attaches to the platform via a second spherical joint. The relative mounting positions of each leg is described in terms of angles ψ_{bi} and ψ_{pi} in the xy plane. γ_i is an angle between ψ_{bi} and the position of the link on the xy base plane, $D1$. Figures 6 and 9 show the coordinates of each leg attachment point.

	Base Connections			Top Connections		
Leg(i)	$b_{xi}(m)$	$b_{yi}(m)$	$b_{zi}(m)$	$p_{xi}(m)$	$p_{yi}(m)$	$p_{zi}(m)$
1	0.0722	0.0277	0	0.0717	0.0205	0
2	0.0277	0.0722	0	0.0205	0.0717	0
3	-0.0277	0.0722	0	-0.0205	0.0717	0
4	-0.0722	0.0277	0	-0.0717	0.0205	0
5	-0.0722	-0.0277	0	-0.0717	-0.0205	0
6	-0.0277	-0.0722	0	-0.0205	-0.0717	0
7	0.0277	-0.0722	0	0.0205	-0.0717	0
8	0.0722	-0.0277	0	0.0717	-0.0205	0

Figure 9: Leg attachment positions to top and base of manipulator base coordinates

The inverse kinematics for this parallel manipulator is calculated to identify goal angles for each of the 8 driven revolute joints around the base platform that will drive the top platform to a desired pose in the manipulator's base coordinates.

[2] Details of the manipulator design including the inverse kinematics were published in Kim, D. and Oh, P.Y., "Towards Lab Automation Drones for Micro-plate Delivery in High Throughput Systems," IEEE International Conference on Unmanned Aircraft Systems, Dallas, TC, June 2018.

The homogeneous transform ${}^{b}T_{p}$ is used to see each leg's attachment point to the top platform, p_i, to its goal pose p^*_i in manipulator's base coordinates

$$p_i{}^* = p_i \, {}^{b}T_{p}$$

Next, the Euclidean distance L^* is calculated as the direct distance between b_i and p^*_i for each leg. L^* is a virtual leg, and it is the hypotenuse of the triangle formed by the points b_i, p^* and the knee, m^*

$$L_i{}^* = \|p_i{}^* - b_i\|$$

Finally, the desired angle of servo rotation, ϑ_i, is calculated by

$$\theta_i = \sin^{-1}\frac{c}{\sqrt{a^2+b^2}} - \tan^{-1}\frac{b}{a}$$

where:

$$a = 2D_1(p_{zi}{}^* - b_{zi})$$

$$b = 2D_1[(p_{zi}{}^* - b_{zi})\cos(\psi_{bi} \pm \gamma_i) + (p_{yi}{}^* - b_{yi})\sin(\psi_{bi} \pm \gamma_i)]$$

$$c = L_i{}^{*2} - D_2^2 + D_1^2$$

In b, the sum of the angles is used in the sinusoids for legs L_1, L_3, L_5, and L_7while the difference of the angles is used for legs L_2, L_4, L_6, and L_8. The net effect was a manipulator that fit within the 4.8 kilogram payload constraints of the selected drone (Diatone Q450).

3.2 Task 2: Smart Gripper (Year 2)

A Vishay VCNL 4010 and ST VL6180X were used to implement a proximity and ambient light sensor. These components provide sensing of up to 200 millimeters and provide size and shape features of objects. These fingernail-sized sensors were embedded in a parallel-jaw gripper designed around a 4-bar linkage.

This gripper (Figure 10) was then mounted on the Stewart-based manipulator (Figure 11) from Year 1. T&E was performed in SISTR (Figure 12).

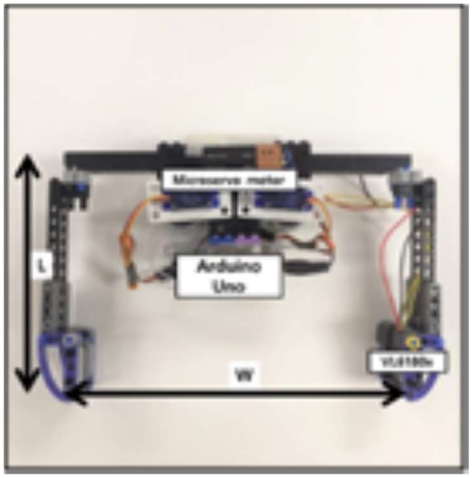

Figure 10 Smart Gripper

Figure 11 Base (white part) for Smart Gripper

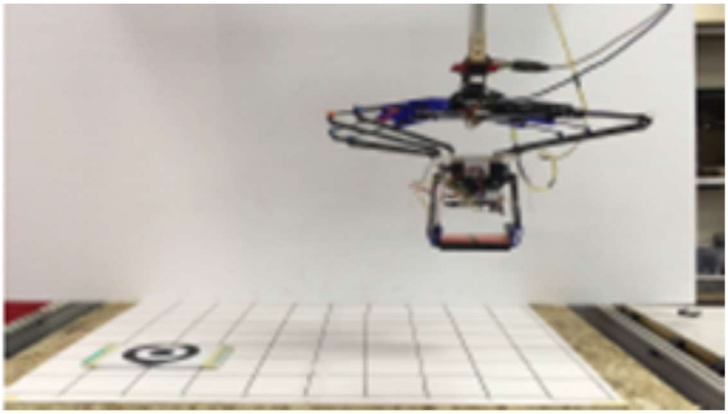

Figure 12 Pick-and-place T&E in SISTR

Envisioning the need to grip hoses for deck cleaning, pick-and-place tasks were initially conducted with the gripper and arm in SISTR (Figure 12). As a sanity check, a light-weight hose (used in aquariums) was then grasped and carried by the aerial manipulator (Figures 13 and 14).

Figure 13: Yellow points to hose. Smart Gripper and arm controlled by pilot

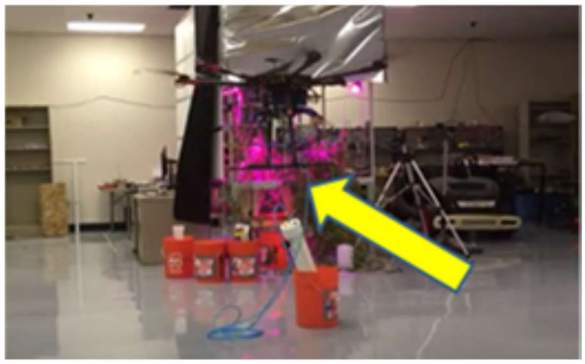

Figure 14: Yellow points to hose. Water supplied from orange buckets

3.3 Task 3: Hosing, Drilling and Epoxying (Year 3)

The continuum of research from prior years was applied to deck cleaning, prepping and repair tasks. As mentioned above, hosing produces a jet stream that could destabilize the drone due to reaction forces and torques on the arm and gripper. The reference frames used are shown in Figure 15. This jetting was modeled to analyze these forces and torques. The model served to define technical design requirements for the aerial manipulator.

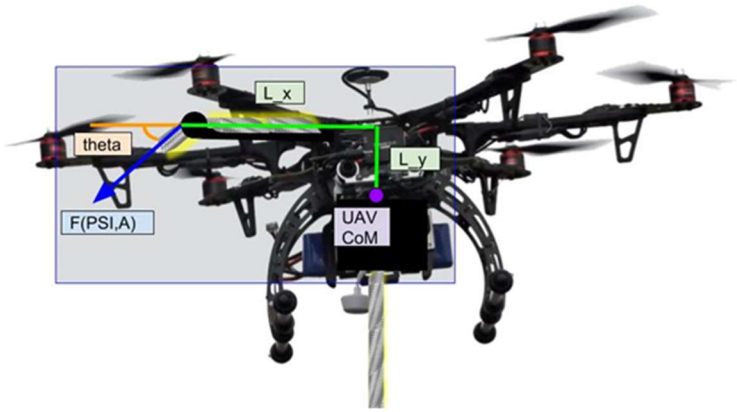

Figure 15: Reference frame for forces and torques

Hose force: The force F_H exerted on a UAV from fluid with density ρ being expelled at velocity v through a hose with area A is modeled as

$$F_H = v\,\frac{dM}{dt} = v(\rho A v) = \rho A v^2 = pA$$

Pressure loss from ground compressor to hose nozzle can be modeled with the Darcy Equation and some additional physical characteristics of the hose: length L, diameter D; and friction factor f_D obtained experimentally. Assuming incompressible flow with velocity v

$$\Delta p = f_D \frac{L}{D}\frac{\rho v^2}{2}$$

Generalized Force and Torque: Consider a hose mounted to a drone. The hose is mounted such that it passes through the vehicle's center of mass (CoM) and remains coplanar with this point as it snakes along the frame to the nozzle mount. Within the shared plane, the nozzle is mounted at some horizontal offset L_x and some vertical offset L_y from the CoM. The nozzle points at some angle θ_n below the horizon, still coplanar with the CoM. This angle depends on the angle from the frame to the nozzle θ_0 and the current pitch of the vehicle θ,

$$\theta_n = \theta_0 + \theta$$

The generalized x and y components of force and perpendicular torque is thus

$$\begin{bmatrix} F_{Hx} \\ F_{Hy} \\ \tau_H \end{bmatrix} = \begin{bmatrix} F_H \cos\theta_n \\ -F_H \sin\theta_n \\ L_y F_H \cos\theta_n + L_x F_H \sin\theta_n \end{bmatrix}$$

The UAV's total available thrust plays an important role in how much hose force can be compensated before actuator saturation occurs and such accelerations are experienced. Given a multi-rotor UAV with an even number n rotors and thrust u_i from each motor mounted at horizontal offset Lx_i from CoM, the generalized x and y components of force and perpendicular torque from the rotors is

$$\begin{bmatrix} F_{Ux} \\ F_{Uy} \\ \tau_U \end{bmatrix} = \begin{bmatrix} \sum u_i \cos\theta_n \\ \sum u_i \sin\theta_n \\ \sum L_x u_i \end{bmatrix}$$

For the case that the drone is constrained to the hose-CoM plane, the above equation can be approximated with a total thrust left and total thrust right of CoM, U_L and U_R respectively, and averaged horizontal motor mount CoM offsets L_{ax}:

$$\begin{bmatrix} F_{Ux} \\ F_{Uy} \\ \tau_U \end{bmatrix} \approx \begin{bmatrix} (\mathrm{U}_L + \mathrm{U}_R)\cos\theta_n \\ (\mathrm{U}_L + \mathrm{U}_R)\sin\theta_n \\ L_{ax}(\mathrm{U}_L - \mathrm{U}_R) \end{bmatrix}$$

Combined Hose-Vehicle Dynamics: To regulate position of a UAV while operating a hose mounted as discussed above, the forces and torque generated by rotor thrust should cancel those of the hose.

$$\begin{bmatrix} \sum F_x \\ \sum F_y \\ \sum \tau \end{bmatrix} = \begin{bmatrix} 0 \\ 0 \\ 0 \end{bmatrix} = \begin{bmatrix} F_{Hx} + F_{Ux} \\ -F_{Hy} + F_{Uy} - Mg \\ \tau_H + \tau_U \end{bmatrix}$$

The net effect is that the Darcy equation was used to calculate the related pressures stemming from the fluid flow in a hose[3]. This served as a basis to define the forces and torques needed in the aerial manipulator to mitigate against the jet stream. The resulting force balance and hose pose (position and orientation) were then analyzed (Figure 16).

[3] Detailed derivations and analysis results published in Hament, B. and Oh, P.Y., "Considerations for Hose-Wielding UAV for Civil Infrastructure Cleaning," 9th International Conference on Structural Health Monitoring of Intelligent Infrastructure, St. Louis, MO, August 2019.

This modeling quantifies bounds on system stability. Assume hose operation begins with low compression pressure, while the vehicle is in a stable hover, and is gradually increased to the desired operating value. If the UAV is to hold position and operate the hose from its initial pose, then the bounds on operation are obtained from solving the force balance in the combined hose-vehicle dynamics.

In initial hardware tests, it was quite clear that the size of the multi-rotor UAV greatly influenced its stability while operating a hose. To probe the theory of this type of behavior, this force balance was evaluated for 3 distinct vehicle configurations:

Vehicle:	**Quad (A)**	**Octo (B)**	**Array (C)**
Mass (kg)	5	15	60
Rotors (n)	4	8	24
Arm Length Mean (m)	.15	.25	.5

The vehicle configurations were selected to represent archetypal small, medium, and large UAV available today. The above table provides more detail on the vehicle masses, frame lengths, and number of rotors. For each vehicle, the tool- space is interrogated with respect to stability along each degree of freedom.

In the 3D surface plots (Figure 3-3-2), the ground plane is the tool-space, permutations of hose pressure and angle. Above the tool-space plane, the surface values represent necessary thrust to maintain position hold. This thrust is color-coded by percentage of total thrust available to the vehicle. Safe operation is denoted by blue and green shading. Possible but risky operation is shaded yellow at 70 % full throttle, orange at 80 %, and light red at 90 %. Theory predicts uncontrollability and instability for

any part of the tool-space with dark red shading overhead, as this would require more than 100 % throttle to compensate for hose reaction forces and torques.

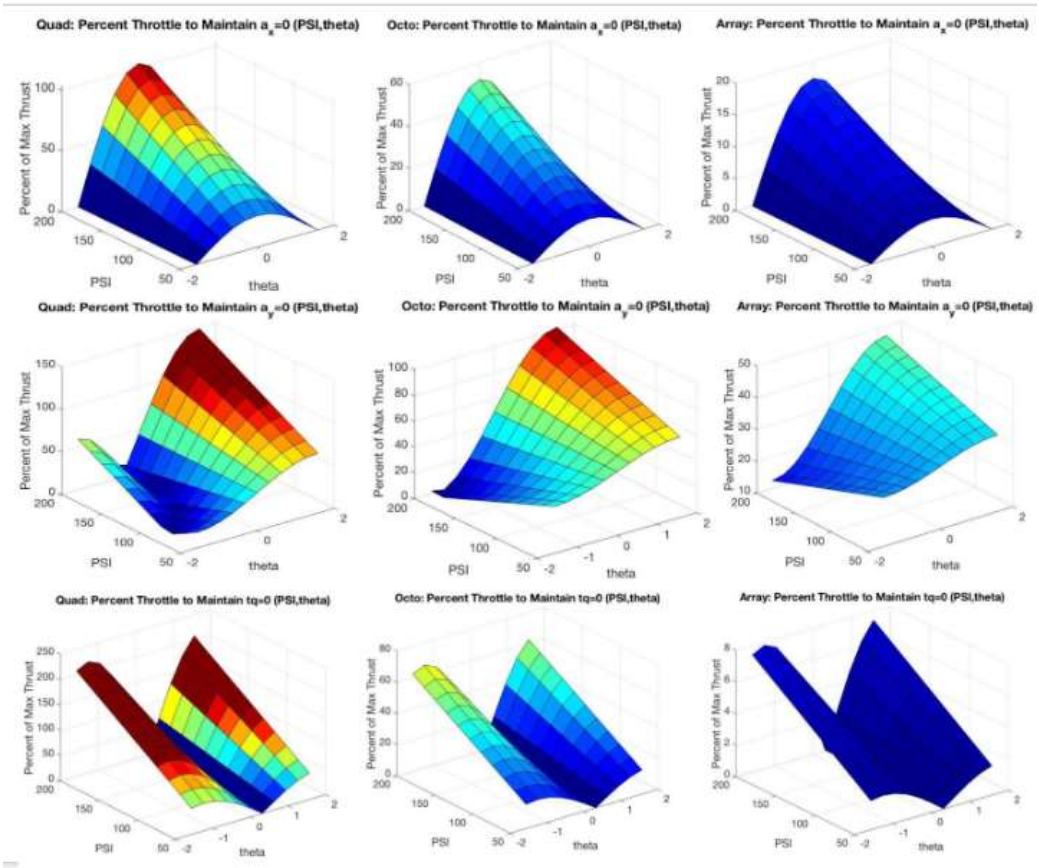

Figure 16: Drone throttle to maintain hose pressure as hose nozzle angle changes).

It is clear from Figure 16 that the larger the vehicle, the larger the available safe tool-space. This is quite intuitive when considering that larger vehicles have more inertia, such that they are less affected by a given hose force and torque than smaller vehicles. Additionally, the larger vehicles have more rotors with which to compensate for hose reaction forces and torques, such that they can counteract the hose at lower percentages of full throttle thrust. Nonetheless, Figure 16 demonstrates that even with a small drone, it is possible to safely operate with very high hose pressures if the hose is mounted strategically. For a given hose pressure and angle, drone designers can adapt hose mounting offsets Lx and Ly to adjust the reaction torque produced by hose. Drone controller designers working with a given aircraft

frame and hose mounting configuration can adjust hose angle θ and vehicle pose in space to safely access high pressures according to the force balances in the combined hose-vehicle dynamics equation.

To demonstrate this, a mock bridge was constructed in the lab (Figures 17and 18) to validate the mitigation of reaction forces and torques. A pneumatic hose set for 100 PSI was carried by the drone. The resulting design effectively blew debris off the deck and sides.

Figure 17: Hosing top of bridge deck

Figure 18: Hosing side of bridge deck

Drilling T&E using the aerial manipulator was also performed. Initial experiments were not very effective. Prior knowledge of the surface's characteristics was needed to set the drill's rotational speed and drill bit insertion force. Without this knowledge, drill bits burned and broke and in some instances destabilized the drone.

A haptic device was then employed. Envisioned was to augment a bridge maintenance worker's skills by providing drilling forces. This is in contrast to a fully autonomous approach; it is more practical to leverage the worker's expertise in drilling to remotely operate the aerial manipulator.

A 6-DOF 3D Touch device was then incorporated into SISTR and calibrated with weight and springs through Hooke's Law (Figures 19 and 20). Force sensing performance was then measured against this

calibration[1]. V&V was then performed in the mo-cap arena to demonstrate untethered aerial manipulation (Figure 21).

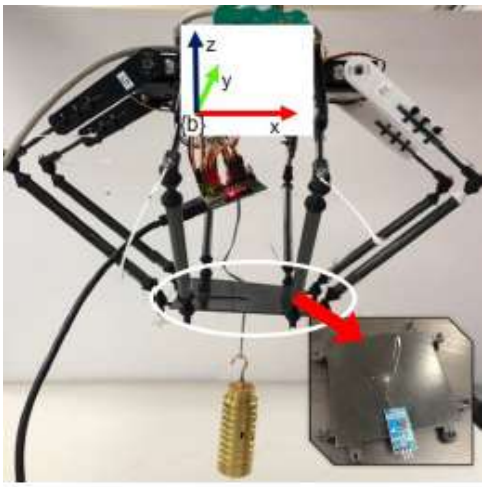

Figure 19: Haptic Sensing Weight Tests

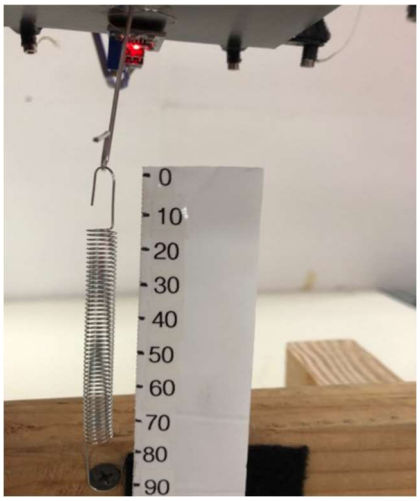

Figure 20: Haptic Sensing Spring Tests

Figure 21: 3D Touch haptic device (right) and provide operator force feedback.

Broadly speaking there are two categories of haptic devices. Admittance-based ones return the corresponding displacement values with force. In contrast, impedance-based ones, like the 3D Touch does the opposite; the corresponding force from displacement measurements is returned. As such,

designing a suitable strain-gauge sensor revolves around the substrate's thickness. The equation that depicts the relationship between the elastic force $F^{\text{spring}}_{\text{total}}$, the spring constant K and displacement x is:

$$F^{\text{spring}}_{\text{total}} = F^{\text{spring}}_{0} + Kx$$

The initial tension force F_0^{spring} captures the spring initial state. The range of calibrated forces is:

$$F^{\text{sensor}}_{\text{min}} \leq F^{\text{sensor}} \leq F^{\text{sensor}}_{\text{max}}$$

A suitable substrate thickness should thus satisfy:

$$F^{\text{sensor}}_{\text{min}} \leq F^{\text{spring}}_{0}$$

The 3D Touch has a 6-DOF stylus. This property allows it to also serve as a joystick to maneuver the drone. This is achieved by first acquiring the scalar force and breaking it down into its three dimensional components

$$\vec{F}_{\text{rendered}} = F_{\text{sensor}}\left(\frac{\vec{r}_{\text{joystick}}}{\|\vec{r}_{\text{joystick}}\|}\right)$$

where

$$\vec{r}_{\text{joystick}} = x_{\text{joystick}}\hat{\imath} + y_{\text{joystick}}\hat{\jmath} + z_{\text{joystick}}\hat{k}$$

and

$$\|\vec{r}_{\text{joystick}}\| = \sqrt{x^2{}_{\text{joystick}} + y^2{}_{\text{joystick}} + z^2{}_{\text{joystick}}}$$

$\vec{r}_{\text{joystick}}$ is position of the joystick provided from haptic device. The 3D Touch's limit switches restrict force measurements to $\pm 3\ N$ in all three dimensions. This was kept in mind by scaling the values returned by the spring.

Haptic manipulation was implemented in SISTR. One end of the spring was fixed to the ground in the gantry's workspace (Figure 19). The operator commanded the arm to grab the spring's free end. The

operator then ascended the arm. Figure 20 shows that the end-effector's position inputs are proportional to the measured forces. These forces were scaled by 50% to avoid triggering the Touch's limit switches. One can also observe that there was a 1 second lag between the force sensor and the 3D Touch. Furthermore, the end-effector position inputs were larger than the spring displacement. This was attributed to the arm's motor torques which were deemed to be slightly underpowered to extend the spring.

Flight trials were conducted. A motion capture marker was placed on the spring to monitor deflection. The operator first commands the drone to take-off and fly to a target location (0, 0, 0.82) in meters. This places the vehicle above the spring. The operator then servos the arm and grabs onto the spring's free end. The spring is stretched when the MMUAV ascends. The operator feels these reaction forces thru the 3D Touch. Figure 22 is an image sequence from recorded video of a flight trial. One observes the similarity of this figure with the one conducted in the gantry. Motion capture data shown in Figures 23 and 24 were used for further evaluation. Flight trials ran for 80 seconds. The spring force was captured and rendered between 63 and 66 seconds. The top graph plots the distance between the drone and spring. The bottom graph plots both the measured and rendered forces and spring displacement measured by motion capture. One also observes that between 63.5 and 64.5 seconds, flight fluctuations cause incorrect for measurements. But once the flight became stable, the measured forces (marked in black) match values from the gantry.

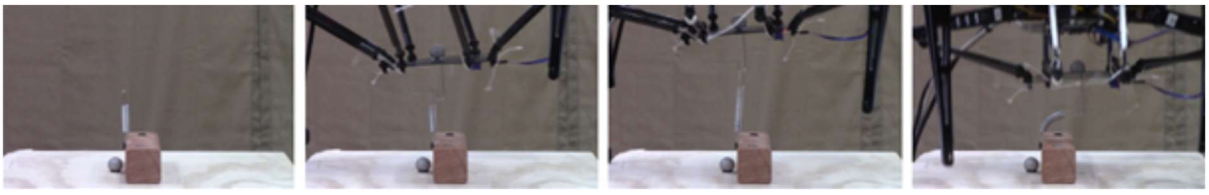

Figure 22: Image sequence of untethered haptic flight of aerial manipulator pulling spring

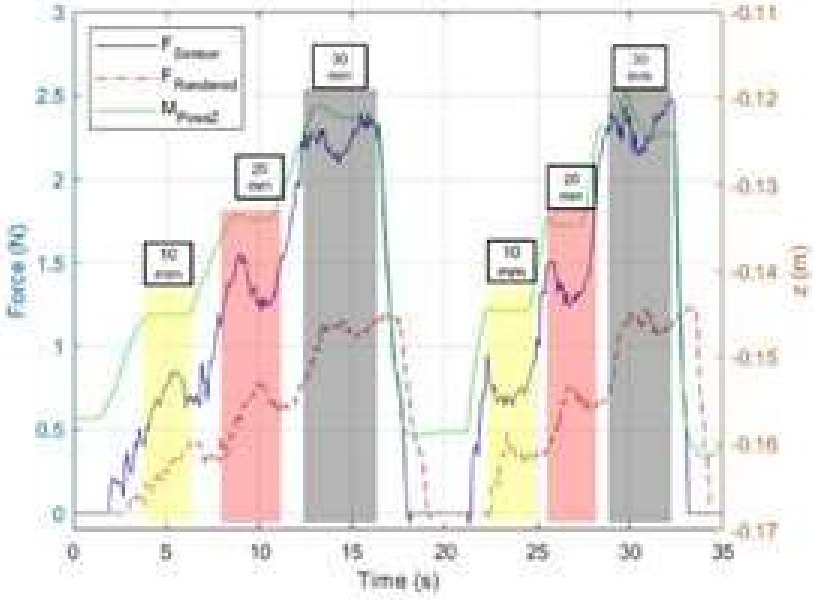

Figure 23: T&E Untethered Flight Tests

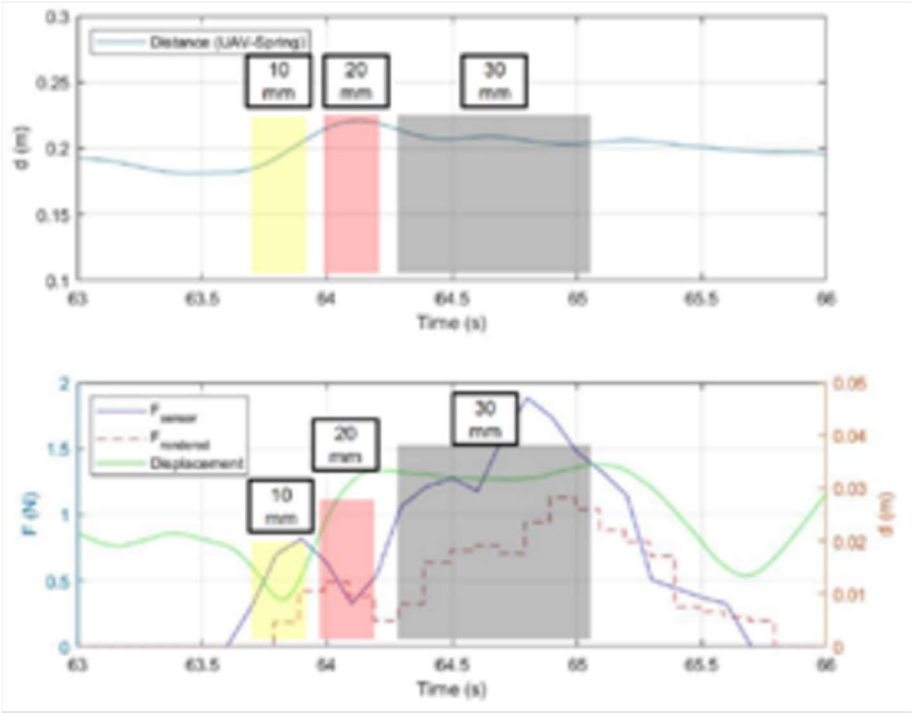

Figure 24: V&V Untethered Flight Tests

4 FINDINGS

The Stewart-based parallel mechanism is a novel design that contrasts serial manipulators used in aerial manipulation. It requires fewer motors (and hence lighter), provides 6-DOF range of motion and has the added benefit of being flatly tucked underneath the drone when not being used. The Smart Gripper showed the ability to embed fingernail-sized sensors in a parallel-jaw gripper to both characterize and grasp objects. Preliminary tests gripping and transporting a hose showed the efficacy of the arm and gripper and performance of the null-space impedance-based controller.

Year 3 applied the continuum of research to actual hosing, drilling and epoxying tasks that characterize bridge deck maintenance. Hosing analysis revealed that reaction forces and torques could be overcome by suitably sizing the drone. This finding reduces the need for a complex stabilizing flight control design; one could use a large high-thrust drone and the resulting moment of inertia would suffice at mitigating the hose's jet stream.

Drilling (and most likely epoxying) is more complex than hosing. Contact forces between the drill bit and surface were found to destabilize the drone. Some experiments resulted in burnt and broken drill bits, and flight failures. The haptics-based approach however showed promise. It is potentially more attractive; a bridge maintenance worker's expertise is used to tele-operate drilling with the aerial manipulator. Rather than promote autonomous operation (and eliminate jobs), this approach augments worker performance and expands their skillset and capabilities.

5 CONCLUSIONS

Aerial manipulation especially for bridge maintenance applications, presents a paradigm shift. Today's drones passively surveil environments. In contrast, aerial manipulation empowers the drone to actively work in such environments by handling objects and operating tools. With hosing, drilling and epoxying tasks in mind, a 6-DOF aerial manipulator and smart gripper were designed and prototyped. The underlying flight controller was used in SISTR and the mo-cap flight arena to test-and-evaluate and verify-and-validate aerial manipulation. Successful hosing was demonstrated on a mock bridge. Drilling revealed limitations of an autonomous approach. However, incorporating haptics and leveraging a bridge maintenance worker's drilling expertise, showed promise. Preliminary results of this approach for maintenance workers to tele-operate a drill carried by the aerial manipulator were conducted. The outcomes point to a human-in-the-loop approach that can be applied broadly to other tasks like epoxying.

6 RECOMMENDATIONS DEVELOPED AS A RESULT OF THIS PROJECT

The research community has focused on autonomous aerial manipulation. Demonstrations include part insertion, hatch opening and valve turning. This project initially began with autonomy in mind and demonstrated tasks like pick-and-place and hose-wielding.

An autonomous robot that performs tasks without human supervision has attraction; workers can be removed from dull, dirty, or dangerous tasks. However, autonomous drilling with aerial manipulators revealed limitations. Moreover, leveraging the maintenance worker's expertise to tele-operate the airborne drill, is more effective and realizable than an autonomous system. This human-in-the-loop aerial manipulation approach is a discovery. When dealing with significant contact forces, the findings show that haptic feedback to an operator can perform drilling. This discovery can broadly apply to other bridge maintenance tasks where there are significant contact forces.

The recommendation is to push this approach by designing a suitable haptics-based drilling system. This system would give the bridge maintenance worker a sense of touch when drilling. Another recommendation is to incorporate immersive optics like virtual-reality and augmented-reality. The net effect would be human-drone interface to remotely work and expedite bridge repairs. Such work can be developed and translate into practice in future years of the project.

7 REFERENCES

Hament, B. and Oh, P.Y., "Considerations for Hose-Wielding UAV for Civil Infrastructure Cleaning," 9th International Conference on Structural Health Monitoring of Intelligent Infrastructure (SHMII-9), St. Louis, MO, pp. 902-907, August 2019.

Kim, D. and Oh, P.Y., "Towards Lab Automation Drones for Micro-plate Delivery in High Throughput Systems," IEEE International Conference on Unmanned Aircraft Systems, Dallas, TC, pp. 279-284, June 2018. DOI: DOI: 10.1109/ICUAS.2018.8453278.

Kim, D. and Oh, P.Y., "Testing-and-Evaluation Platform for Haptics-based Aerial Manipulation with Drones," American Control Conference (ACC), Denver, CO, July 2020 (accepted). No DOI number yet. Will be published/archived in IEEE Xplore.